

Highly efficient double-doped solid-state white light-emitting electrochemical cells

Hai-Ching Su,^{*a} Hsiao-Fan Chen,^b Yu-Chun Shen,^a Chih-Teng Liao^a and Ken-Tsung Wong^{*b}

Received 1st February 2011, Accepted 21st April 2011

DOI: 10.1039/c1jm10507h

We report highly efficient, solid-state, white light-emitting electrochemical cells (LECs) based on a double-doped strategy, which judiciously introduces an orange-emitting guest, $[\text{Ir}(\text{ppy})_2(\text{dasb})]^+(\text{PF}_6^-)$, into a single-doped emissive layer comprised of an efficient blue-green emitting host, $[\text{Ir}(\text{dfppz})_2(\text{dtb-bpy})]^+(\text{PF}_6^-)$, and a red-emitting guest, $[\text{Ir}(\text{ppy})_2(\text{biq})]^+(\text{PF}_6^-)$, to improve the balance of carrier mobilities and, thus, to enhance the device efficiency. Photoluminescence (PL) measurements show that the single-doped (red guest) and the double-doped (red and orange guests) host-guest films exhibit similar white PL spectra and comparable photoluminescence quantum yields, while the device efficiencies of the double-doped white LECs are twofold higher than those of the single-doped white LECs. Therefore, such enhancement of the device efficiency is rationally attributed to the improved balance of carrier mobilities of the double-doped emissive layer. Peak external quantum efficiency and peak power efficiency of the double-doped white LECs reached 7.4% and 15 lm W^{-1} , respectively. These efficiencies are amongst the highest reported for solid-state white LECs and, thus, confirm that the double-doping strategy is useful for achieving highly efficient white LECs.

Introduction

White organic light-emitting diodes (OLEDs) based on polymers and small-molecule materials have attracted intense attention due to their potential applications in flat-panel displays and solid-state lighting.¹⁻⁴ Compared with conventional white OLEDs,^{5,6} solid-state white light-emitting electrochemical cells (LECs)⁷ possess several promising advantages. LECs generally require only a single emissive layer, which can be easily processed from solutions, and, conveniently, can use air-stable electrodes. The emissive layer of LECs contains mobile ions, which can drift toward electrodes under an applied bias. The spatially separated ions induce electrochemical doping (oxidation and reduction) of the emissive materials near the electrodes, *i.e.* p-type doping near the anode and n-type doping near the cathode.⁷ The doped regions induce ohmic contacts with the electrodes and consequently facilitate the injection of both holes and electrons, which recombine at the junction between the p- and n-type regions. As a result, a single-layered LEC device can be operated at very low voltages (close to E_g/e , where E_g is the energy gap of the emissive material and e is elementary charge) with balanced carrier injection, giving high power efficiencies. Furthermore, air-stable metals, *e.g.* Au and Ag, can be used, since carrier injection in

LECs is relatively insensitive to the work functions of the electrodes.

Solid-state white LECs based on a phase-separated polyfluorene/poly(ethylene oxide) (PEO) mixture, exhibiting an external quantum efficiency (EQE) of 2.4% photons/electron, were reported by Yang *et al.* in 1997.⁸ Recently, white LECs based on excimer emission of a fluorene-oxadiazole copolymer with a current efficiency of 0.15 cd A^{-1} have been reported by Sun *et al.*⁹ However, moderate efficiencies of polymer LECs showed that the fluorescent nature of conjugated polymers limits the eventual electroluminescence (EL) efficiency due to the spin statistics. To improve device efficiencies, phosphorescent cationic transition metal complexes (CTMCs) have been intensively studied for use in solid-state LECs.¹⁰⁻⁵⁰ Furthermore, compared to conventional polymer LECs, no ion-conducting material (*e.g.* PEO) is needed in CTMC-based LECs, since CTMCs are intrinsically ionic. By employing a blue-green-emitting CTMC as the host and a red-emitting CTMC as the guest, solid-state white LECs with an EQE (power efficiency) of 4% (7.8 lm W^{-1}) were successfully demonstrated by Su *et al.* in 2008.³⁵ Recently, improving the EQE (power efficiency) of single-doped CTMC-based white LECs up to 5.6% (11.2 lm/W) has been achieved by He *et al.*^{41,45} However, further improving the device efficiency of white LECs is still required for practical applications.

Enhancing the device efficiency of CTMC-based host-guest white LECs can be realized by utilizing efficient CTMCs and by improving the balance of carrier mobilities of devices. An efficient blue-green emitting host, with superior steric hindrance to avoid self-quenching in the condensed phase, and corresponding

^aInstitute of Lighting and Energy Photonics, National Chiao Tung University, Tainan, 71150, Taiwan. E-mail: haichingsu@mail.nctu.edu.tw; Fax: +886-6-3032535; Tel: +886-6-3032121-57792

^bDepartment of Chemistry, National Taiwan University, Taipei, 10617, Taiwan. E-mail: kenwong@ntu.edu.tw; Fax: +886-2-33661667; Tel: +886-2-33661665

efficient red emitting guests doped in host films to generate efficient white emission are required to enhance the device efficiency. On the other hand, the balance of carrier mobilities of host–guest white LECs can be modified by varying the doping concentrations of the guests, since offsets in the energy levels of the host and guest molecules would induce carrier trapping and, thus, alter the carrier mobilities of the host films. However, tuning the doping concentration of the guest in single-doped white LECs would simultaneously alter the white EL spectra, possibly resulting in a significant color shift. In this work, we propose a double-doping strategy, which additionally introduces an efficient orange-emitting CTMC into a single-doped emissive layer containing an efficient blue–green-emitting host and a red-emitting guest, to improve the balance of the carrier mobilities and, thus, to enhance the device efficiency of white LECs. Photoluminescence (PL) measurements show that the single-doped (red guest) and the double-doped (red and orange guests) host–guest films exhibit similar white PL spectra and comparable photoluminescence quantum yields (PLQYs), while device efficiencies of the double-doped white LECs are twofold higher than those of the single-doped white LECs. Therefore, such enhancement of the device efficiency is rationally attributed to the improved balance of the carrier mobilities of the double-doped emissive layer. Peak EQE and power efficiency of the double-doped white LECs reach 7.4% and 15 lm W⁻¹, respectively. These efficiencies are amongst the highest reported for white LECs and confirm that the double-doping strategy is a useful technique for enhancing the device efficiencies of white LECs.

Results and discussion

Photophysical studies

The chemical structures of the host and guest materials used in this study are shown in Fig. 1. All of the complexes were synthesized according to the procedures reported in the literature.^{23,30,35} The blue–green-emitting cationic Ir complex

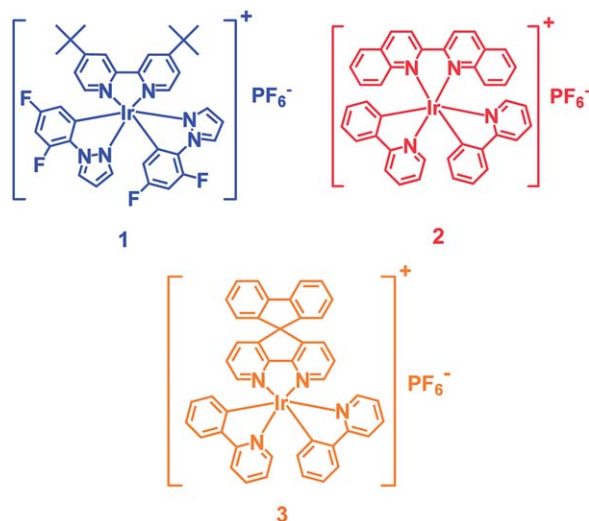


Fig. 1 Molecular structures of [Ir(dfppz)₂(dtb-bpy)]⁺(PF₆⁻) (**1**), [Ir(ppy)₂(biq)]⁺(PF₆⁻) (**2**) and [Ir(ppy)₂(dasb)]⁺(PF₆⁻) (**3**).

[Ir(dfppz)₂(dtb-bpy)]⁺(PF₆⁻) (**1**), where dfppz is 1-(2,4-difluorophenyl)pyrazole and dtb-bpy is [4,4'-di(*tert*-butyl)-2,2'-bipyridine], reported previously by Tamayo *et al.*²³ was used as the host. [Ir(ppy)₂(biq)]⁺(PF₆⁻) (**2**), where ppy is 2-phenylpyridine and biq is 2,2'-biquinoline, which was used as the red-emitting complex in white LECs reported by Su *et al.*,³⁵ was utilized as the red-emitting guest. Efficient orange-emitting [Ir(ppy)₂(dasb)]⁺(PF₆⁻) (**3**), where dasb is 4,5-diaza-9,9'-spirobifluorene, utilized as the guest in host–guest LECs to achieve an EQE >10%³¹ was chosen as the additional guest for modifying the balance of the carrier mobilities and, thus, enhancing the device efficiency of the white LECs. The photophysical properties of complexes **1–3** in solution (dichloromethane, 10⁻⁵ M) and in thin films are summarized in Table 1. The PL spectra of complexes **1–3** in solution (dichloromethane, 10⁻⁵ M) and in neat films are shown in Fig. 2. Complex **1** shows approximately the same blue–green PL emission in solution and in neat films, which may be associated with the reduced intermolecular interactions induced by the sterically bulky di-*tert*-butyl groups of the bipyridine ligand.²³ The highly retained PLQY of **1** in neat films (0.75) in comparison with that in solutions (1.00) further confirms the reduced self-quenching in neat films, resulting from the sterically bulky ligand of **1**, suggesting its suitability for use as the host of white LECs (Table 1). Complex **2** exhibits saturated red PL emission in both solution and neat films and, thus, is suitable for use as the red-emitting guest of white LECs.³⁵ Complex **3** possesses orange PL emission covering part of the red spectrum in solution and in neat films. Therefore, replacing some portion of **2** in a host(**1**)–guest(**2**) film with a proper concentration of **3** would not significantly change the white PL spectrum. However, the balance of the carrier mobilities of the host–guest film would be altered in this way due to a modified carrier trapping effect induced by the discrepancy between the energy levels of **2** and **3**.

To study the effects of replacing some portion of **2** in host(**1**)–guest(**2**) films with **3** on the PL emission properties, the photophysical characteristics of the single-doped [**2** (0.2 wt.%) and the double-doped [**2** (0.05 wt.%) and **3** (0.1 wt.%) host–guest films were measured and are summarized for comparison in Table 1. As shown in Fig. 3, these doping concentrations were chosen so that both the single-doped and the double-doped films show a similar amount of red PL emissions ($\lambda > 600$ nm) when the intensities of their blue–green PL emission peaks are normalized to comparable values. Although the concentration of the red-emitting guest (**2**) is lower in the double-doped films (0.05 wt.%), additional red PL emission, provided by the orange-emitting guest (**3**) in the double-doped films, enhances the total red PL emission to be comparable to that obtained in the single-doped films containing a higher concentration of **2** (0.2 wt.%). A slightly higher PLQY of the double-doped films (0.64) in comparison with that of the single-doped films (0.61) further confirms the partial contribution of red PL emission from **3**, since **3** is more efficient than **2** at low doping concentrations (Table 1). These results reveal that the white PL spectra of the double-doped films can be tuned to resemble those of the single-doped films by adjusting the doping concentrations of the two guests. Meanwhile, the balance of the carrier mobilities of the single-doped films, which is affected by carrier trapping induced by offsets in the energy levels of the host and guest molecules, would,

Table 1 A summary of the photophysical properties of 1–3

Complex	$\lambda_{\text{max, PL}} (\text{nm})^a, \Phi^b$		
	Solution ^c	Neat film or host–guest film	Film with BMIM ⁺ (PF ₆ ⁻) ^d
1	492, 1.00	492, 0.75	—
2	656, 0.20	672, 0.09	—
3	558, 0.52	593, 0.32	—
2 (0.2 wt.%): 1	—	(487, 600), 0.61	(485, 598), 0.64
2 (0.05 wt.%) and 3 (0.1 wt.%): 1	—	(506, 592), 0.64	(505, 592), 0.69

^a Peak or shoulder wavelength of PL spectra. ^b Photoluminescence quantum yields. ^c Measured in dichloromethane (10⁻⁵ M). ^d Films containing 20 wt.% BMIM⁺(PF₆⁻).

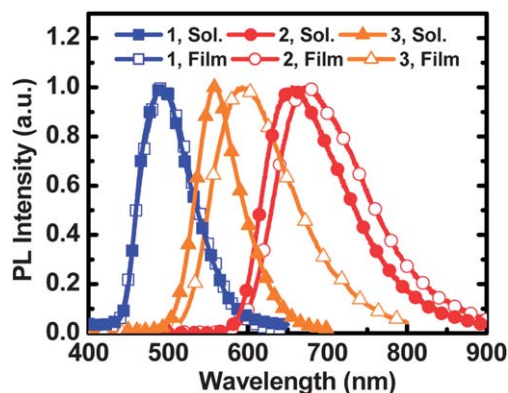


Fig. 2 PL spectra of 1–3 in dichloromethane solution (10⁻⁵ M) and in neat films.

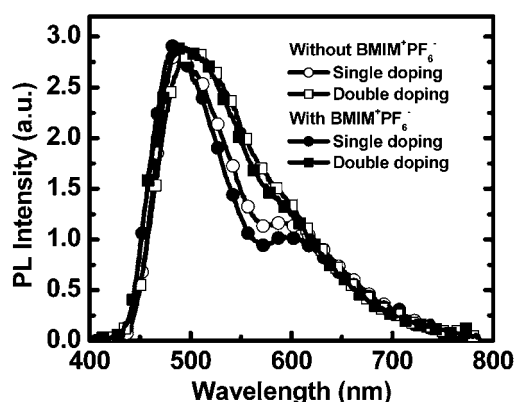


Fig. 3 PL spectra of the single-doped [2 (0.2 wt.%) and the double-doped [2 (0.05 wt.%) and 3 (0.1 wt.%) host–host films with and without BMIM⁺(PF₆⁻) (20 wt.%).

therefore, be modified by introducing an additional guest. Since in LECs, an ionic liquid BMIM⁺(PF₆⁻) (where BMIM is 1-butyl-3-methylimidazolium) of 20 wt.% was added to provide additional mobile ions and to shorten the device response time,²¹ the photophysical properties of the BMIM⁺(PF₆⁻) blended host–guest films were also characterized and are summarized in Table 1. With the presence of BMIM⁺(PF₆⁻), both the single-doped and the double-doped films show slightly blue-shifted PL spectra and slightly higher PLQYs (Table 1), indicating the role of BMIM⁺(PF₆⁻) in suppressing intermolecular interactions.³¹

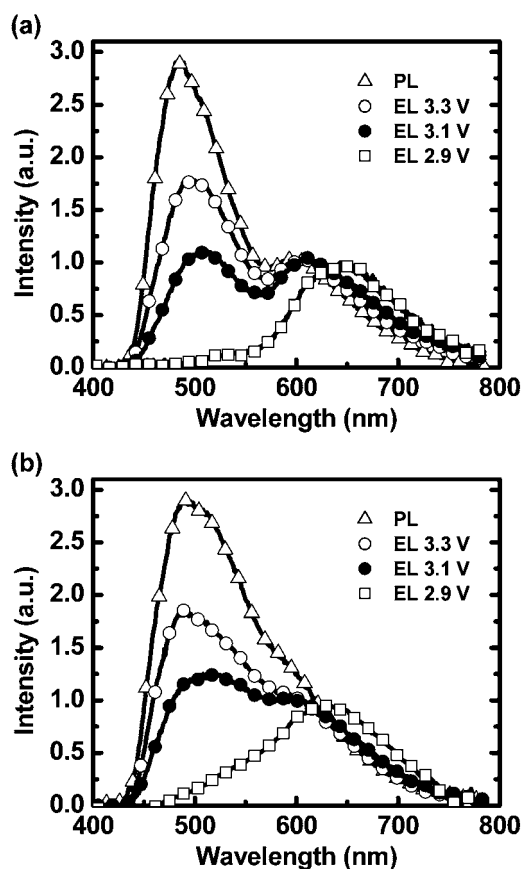
EL characteristics of white LECs

To clarify the modified balance of the carrier mobilities of the double-doped films in comparison with that of the single-doped films, EL characteristics of white LECs based on single- and double-doped emissive layers were measured and are summarized in Table 2. The white LECs have the structure of indium tin oxide (ITO)/poly(3,4-ethylenedioxythiophene):poly(styrene sulfonate) (PEDOT:PSS) (30 nm)/emissive layer (200 nm)/Al (100 nm), where the emissive layer contains 1 (79.8 wt.%), 2 (0.2 wt.%), and BMIM⁺(PF₆⁻) (20 wt.%) for the single-doped Device I and 1 (79.85 wt.%), 2 (0.05 wt.%), 3 (0.1 wt.%) and BMIM⁺(PF₆⁻) (20 wt.%) for the double-doped Device II. The ionic liquid, BMIM⁺(PF₆⁻) of 20 wt.%, was added to provide additional mobile ions and to shorten the device response time.²¹ The EL spectra of Device I and Device II under various biases, along with the PL spectra of the emissive layers for comparison, are shown in Figs 4(a and b), respectively. Compared with PL, the relative intensity of the orange and red emission with respect to the blue–green emission is larger in EL and increases as the bias decreases for both devices. Similar phenomena were also observed in previously reported white LECs based on host–guest CTMCs.^{35,41} This could be understood by energy level alignments (estimated by cyclic voltammetry) of the host and guests shown in Fig. 5.^{23,31,35} For host–guest white LECs, electrochemically doped regions of the emissive layer result in ohmic contact with the metal electrodes and, consequently, facilitate carrier injection onto both the host and the guest. Hence, both exciton formation on the host followed by host–guest energy transfer and direct exciton formation on the guest, induced by charge trapping, contribute to the guest emission. At lower biases, such energy level alignments (Fig. 5) favor carrier injection and trapping on the smaller gap guests (2 and 3), resulting in direct carrier recombination/exciton formation on the guest (rather than host–guest energy transfer). For guest 3, the host–guest energy offset in the highest occupied molecular orbital (HOMO) levels (0.37 eV) is much larger than that in the lowest unoccupied molecular orbital (LUMO) levels (0.07 eV). Guest 3 would, therefore, lead to more significant hole trapping than electron trapping, altering the balance of the carrier mobilities of the emissive layer. Furthermore, direct exciton formation on guest 3 would take place due to carrier trapping. On the other hand, for the guest 2, comparable large host–guest energy offsets in the HOMO (0.39 eV) and the LUMO levels (0.46 eV) would result in more pronounced hole and electron trapping and, consequently, more significant direct exciton formation on guest 2. Therefore,

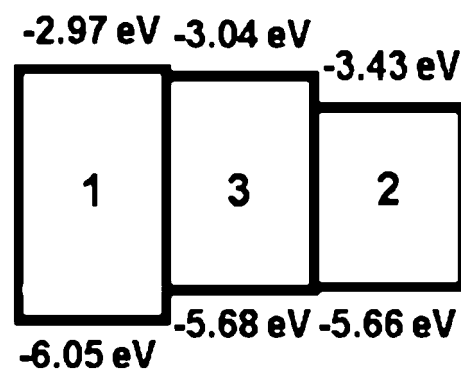
Table 2 A summary of the EL characteristics of white LECs

Device ^a	Bias (V)	CIE (x, y) ^b	CRI ^b	t _{max} (min) ^c	L _{max} (cd m ⁻²) ^d	η _{ext, max} , η _{L, max} , η _{p, max} (%), (cd A ⁻¹ , lm W ⁻¹) ^e	t _{1/2} (min) ^f
I	2.9	(0.576, 0.382)	— ^g	397	0.2	(1.7, 1.7, 1.9)	1312 ^h
	3.1	(0.391, 0.440)	83	95	3.7	(3.2, 5.4, 5.4)	227
	3.3	(0.328, 0.423)	76	80	6.0	(3.2, 6.2, 5.9)	102
II	2.9	(0.532, 0.444)	84	280	1.2	(5.6, 9.2, 10.0)	446 ⁱ
	3.1	(0.365, 0.451)	75	60	11.5	(7.4, 14.8, 15.0)	120
	3.3	(0.318, 0.427)	70	29	20.2	(6.3, 13.4, 12.8)	37

^a ITO/PEDOT:PSS (30 nm)/emissive layer (200 nm)/Al (100 nm), where the emissive layer contains **1** (79.8 wt.%), **2** (0.2 wt.%), and BMIM⁺(PF₆⁻) (20 wt.%) for Device I and **1** (79.85 wt.%), **2** (0.05 wt.%), **3** (0.1 wt.%) and BMIM⁺(PF₆⁻) (20 wt.%) for Device II. ^b Evaluated from the EL spectra. ^c Time required to reach the maximum brightness. ^d Maximal brightness achieved at a constant bias voltage. ^e Maximal external quantum efficiency, current efficiency and power efficiency achieved at a constant bias voltage. ^f The time for the brightness of the device to decay from the maximum to half of the maximum under a constant bias voltage. ^g Undefined CRI for this spectrum. ^h Extrapolated.

**Fig. 4** The EL spectra of (a) Device I and (b) Device II under various biases compared with the PL spectra of the emissive layers.

larger fractions of guest emission, especially for **2** are observed at lower biases. However, white EL emission with Commission Internationale de l'Éclairage (CIE)⁵¹ coordinates of (0.328, 0.423) and (0.318, 0.427) could be achieved at higher biases for Device I and Device II, respectively (Table 2). Furthermore, both of the white LECs, under 3.1–3.3 V, exhibit good color rendering indices (CRI) (>70),⁵² which are essential for solid-state lighting. It is noted that, compared with the EL emission of single-doped Device I, that of double-doped Device II containing **3** shows an enhanced intensity in the yellow spectrum (around 550 nm) (Fig. 4) and thus renders higher lumen values due to better

**Fig. 5** The energy level diagram of the host (**1**) and guest (**2** and **3**) molecules.

matching between its EL spectrum and the luminosity function.⁵³ Such EL emission characteristic of the double-doped Device II may be advantageous in raising the power efficiency (lm/W), which is an important figure of merit of white light-emitting devices for solid-state lighting.

The time-dependent brightness and current density under constant biases of 2.9–3.3 V for Device I and Device II are shown in Figs 6(a and b), respectively. Both devices showed a similar trend in the time-dependent brightness and current density. After the bias was applied, the current first rose and then stayed rather constant. On the other hand, the brightness first increased with the current and reached maxima of 0.2, 3.7 and 6.0 cd m⁻² for Device I and 1.2, 11.5 and 20.2 cd m⁻² for Device II under biases of 2.9, 3.1 and 3.3 V, respectively. The brightness then dropped with time, with a rate depending on the bias voltage (or current). The corresponding time-dependent EQEs and power efficiencies of Device I and Device II are shown in Fig. 7(a and b), respectively. When a forward bias was applied, the EQE was rather low due to poor carrier injection. During the formation of the doped regions near the electrodes, the capability of the carrier injection was improved and, thus, the EQE rose rapidly. The peak EQEs, current efficiencies and power efficiencies are (1.7%, 1.7 cd A⁻¹, 1.9 lm W⁻¹), (3.2%, 5.4 cd A⁻¹, 5.4 lm W⁻¹) and (3.2%, 6.2 cd A⁻¹, 5.9 lm W⁻¹) for Device I and (5.6%, 9.2 cd A⁻¹, 10.0 lm W⁻¹), (7.4%, 14.8 cd A⁻¹, 15.0 lm W⁻¹) and (6.3%, 13.4 cd A⁻¹, 12.8 lm W⁻¹) for Device II at 2.9, 3.1 and 3.3 V, respectively (Table 2). The device efficiencies of single-doped Device I are similar to

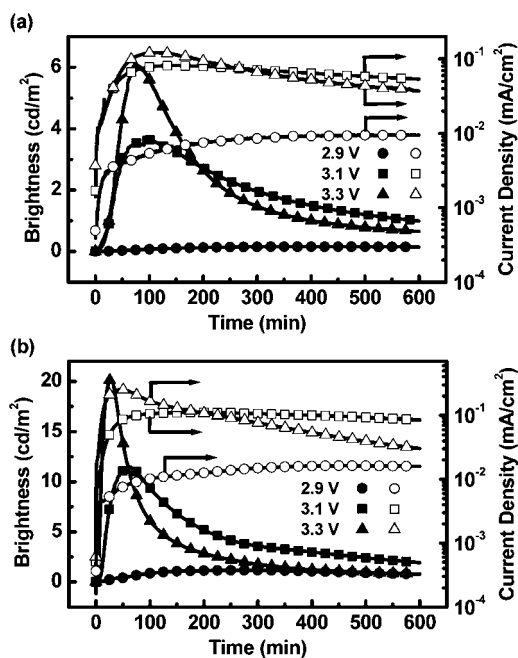


Fig. 6 The brightness (solid symbols) and current density (open symbols) as a function of time under a constant bias voltage of 2.9–3.3 V for (a) Device I and (b) Device II.

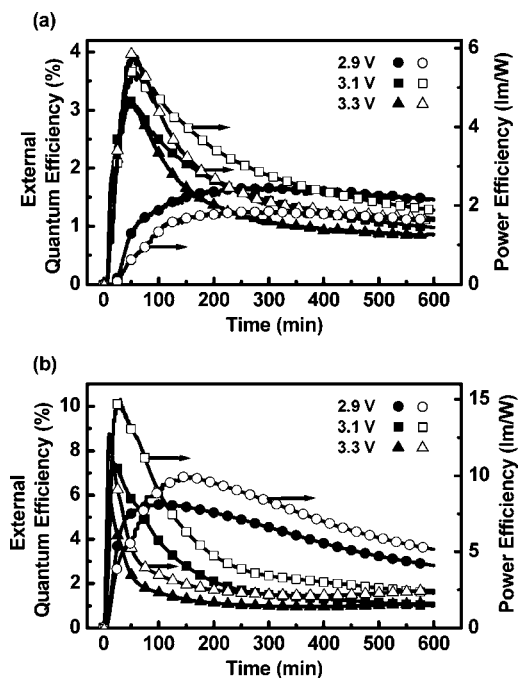


Fig. 7 The external quantum efficiency (solid symbols) and power efficiency (open symbols) as a function of time under a constant bias voltage of 2.9–3.3 V for (a) Device I and (b) Device II.

those of previously reported single-doped CTMC-based white LECs.³⁵ On the other hand, the device efficiencies of double-doped Device II are twofold higher than those of single-doped Device I and are among the highest reported for white LECs.^{8,9,35,41,45} The significantly enhanced device efficiencies of

double-doped (2 and 3) Device II in comparison to those of single-doped (2) Device I confirm that the addition of a CTMC (3) improves the balance of the carrier mobilities of white LECs, since the emissive layers of both devices show similar PLQYs (Table 1) and the doped regions near the electrodes of the LECs ensure balanced carrier injection.^{7–50} As the carrier injection at both electrodes becomes balanced, the carrier recombination zone may consequently locate near one of the electrodes due to discrepancies in the electron and hole mobilities of the emissive layer. The recombination zone in the vicinity of an electrode may cause exciton quenching such that the EQE of the device would decrease. Balanced electron and hole mobilities would be beneficial in keeping the recombination zone near to the center of the emissive layer and, thus, would prevent exciton quenching, enhancing the device efficiency. The measured EQE of single-doped Device I (3.2%) is much lower than that (*ca.* 13%) estimated from the PLQY of its emissive layer (0.64, Table 1) when considering a perfect balance of carrier mobilities and a $\sim 20\%$ optical outcoupling efficiency from a typical layered light-emitting device structure. It implies a poor balance of the carrier mobilities in the emissive layer of single-doped Device I. The single-doped films possessing a slightly larger energy offset in the LUMO levels (0.46 eV) than in the HOMO levels (0.39 eV) between the host (1) and guest (2) may lead to more pronounced electron trapping and, thus, would reduce the ratio of the electron to hole mobility compared to neat host films (Fig. 5). Compared with the single-doped films, a much smaller energy offset in the LUMO levels (0.07 eV) between 1 and 3 (Fig. 5) may reduce electron trapping in the double-doped films in which part of 2 is replaced with 3 and, consequently, would increase the ratio of the electron to hole mobility, producing an opposite adjustment of the balance of the carrier mobilities with respect to the single-doped films. Such a modification in the balance of the carrier mobilities results in considerable enhancement of the EQE of double-doped Device II (7.4%). These results confirm that the device efficiencies of the single-doped white LECs can be significantly improved through tailoring the balance of the carrier mobilities induced by adding a second guest with the proper energy levels. The drop in efficiencies and brightness after reaching the peak value, as commonly seen in solid-state LECs,^{7–50} may be attributed to a few factors. Before the current reaches a steady value, the carrier recombination zone may keep moving closer to one electrode due to discrepancies in the electron and hole mobilities, which would induce exciton quenching. Furthermore, the decrease in the brightness and efficiencies under a constant bias was irreversible and, thus, may be rationally associated with the degradation of the emissive material during the LEC operation.¹⁵

The peak brightness and turn-on time (the time required to reach the maximal brightness) as a function of bias voltage for both white LECs are shown in Fig. 8(a). An electrochemical junction between p- and n-type doped layers of LECs is formed during device operation. As the bias voltage increases, the junction width decreases due to extension of the doped layers,¹⁷ consequently leading to a higher current density and a higher brightness (Fig. 6). Device I exhibited a lower peak brightness than Device II under the same bias voltage due to a lower current density (Fig. 6) and a lower device efficiency (Fig. 7). The lower current density of Device I is attributed to more pronounced

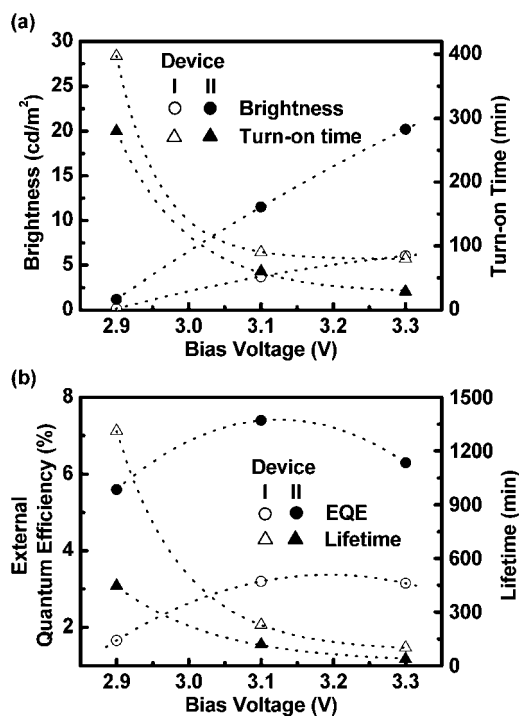


Fig. 8 (a) The peak brightness (circles) and turn-on time (triangles) and (b) the peak external quantum efficiency (circles) and lifetime (triangles) as a function of the bias voltage for Device I (open symbols) and Device II (solid symbols).

carrier trapping induced by smaller-gap guests (2) at a higher doping concentration (Fig. 5). The higher electric field in the device induced by a higher bias voltage accelerates the redistribution of mobile ions, which facilitates the formation of ohmic contacts with the electrodes and, thus, quickens the device response (Fig. 8(a)). The less pronounced carrier trapping of Device II increases the effective bias voltage across the device and, consequently, leads to a higher electric field, producing a faster device response compared to Device I under the same bias voltage (Fig. 8(a)). A higher brightness and faster response are obtained at the expense of device stability. As shown in Fig. 8(b), the peak EQE and device lifetime (the time for the brightness of the device to decay from the maximum to half of the maximum under a constant bias voltage) of both of the white LECs deteriorate under a high bias voltage (3.3 V). This may be associated with the higher electric field or current density accelerating the degradation (multiple oxidation and subsequent decomposition)²¹ of the CTMC. It is noted that the lower EQEs obtained in both white LECs at 2.9 V result from the predominant red EL spectra (Fig. 4), which exhibit lower EL efficiencies. Compared with Device II, Device I exhibits lower current densities and, thus, lower degradation rates, resulting in longer device lifetimes (Fig. 8(b)). Detailed degradation mechanisms of white LECs based on CTMCs remain unclear and further studies are still needed to achieve practical device lifetimes.

To clarify the importance of this work, we compare our results with those published in previous literature. Several previous demonstrations of solid-state white LECs based on host-guest CTMCs have been reported to exhibit moderate EQEs (4–5.6%).^{35,41,45} All of them are single-doped devices, which are

composed of a blue-green emitting host doped with a red-emitting guest. The doping concentration of the guest was chosen to appropriately tune the energy transfer rate to achieve a good quality white EL spectrum, e.g., a proper CIE coordinate and a high CRI. However, the balance of the carrier mobilities (and, thus, the device efficiency) and the quality of the white EL of the single-doped devices would not generally be optimized simultaneously by tuning the doping concentration of a single guest, which concurrently affects carrier trapping and energy transfer. Such a phenomenon was revealed in previous reports on single-doped white LECs, for example, in ref. 41 and ref. 45. The PLQYs (in acetonitrile solutions) of the host materials and the EQEs of the host-only LECs used in ref. 41 and ref. 45 are (0.24, 3.4%) and (0.54, 7.6%), respectively.^{41,45} Enhancement of the EL efficiency of the host material used in ref. 45 compared to that used in ref. 41 (2.24 times) predominately results from improvement of the PLQY of the host material (by 2.25 times). This, therefore, implies a similar degree of balance of the carrier mobilities of both host materials. However, when doped with the same red-emitting guest, enhancement of the EQEs of the white LECs in ref. 45 (5.6%), compared to those in ref. 41 (5.2%), is only *ca.* 8%, which is much lower than the improvement in the EQEs of the corresponding host-only LECs (224%).^{41,45} These results indicate that the altered balance of the carrier mobilities induced by the guest dominates the EQE of the single-doped white LECs, even when they contain an efficient host, precluding further enhancement of the device efficiencies. Therefore, a double-doping strategy to simultaneously achieve good-quality white EL and improvement of the balance of the carrier mobilities is required to enhance the device efficiencies of host-guest white LECs. However, to the best of our knowledge, no such demonstration has yet been reported. In this work, we propose a double-doping strategy, which additionally introduces an orange-emitting CTMC into a single-doped emissive layer containing an efficient blue-green emitting host and a red-emitting guest, to improve the balance of the carrier mobilities and, thus, to enhance the device efficiency of white LECs. Compared with the single-doped white LECs, the EQEs of the double-doped white LECs (7.4%) were indeed significantly enhanced and these results are better than those of previously reported single-doped white LECs.^{35,41,45} Thus, the research results of this work successfully demonstrate a novel technique for enhancing the device efficiencies of white LECs.

Conclusions

In summary, we have reported efficient solid-state white LECs based on a double-doping strategy, which introduces an orange-emitting guest (3), [Ir(ppy)₂(dasb)]⁺(PF₆⁻) along with a red-emitting guest (2), [Ir(ppy)₂(biq)]⁺(PF₆⁻) in an emissive layer containing an efficient blue-green emitting host (1), [Ir(dfppz)₂(dtb-bpy)]⁺(PF₆⁻). PL measurements show that the single-doped (2) and the double-doped (2 and 3) host-guest films exhibit similar white PL spectra and comparable PLQYs, while the device efficiencies of the double-doped white LECs are twofold higher than those of the single-doped white LECs. Therefore, such an enhancement of the device efficiency is rationally attributed to an improved balance of the carrier mobilities of the double-doped emissive layer. The peak EQE

and peak power efficiency of the double-doped white LECs reached 7.4% and 15 lm W⁻¹, respectively. These efficiencies are among the highest reported for white LECs and confirm that the double-doping strategy is a useful technique for realizing highly efficient white LECs.

Experimental

Photophysical measurements

Photophysical characteristics of **1–3** in solution were collected at room temperature by using 10⁻⁵ M dichloromethane solutions of all complexes, which were carefully purged with nitrogen prior to measurements. The neat films of **1–3** and mixed host–guest films for photophysical studies were spin-coated at 3000 rpm onto quartz substrates (1 × 0.5 cm²) using mixed solutions (in acetonitrile) of various ratios. The mass ratios of the solute component (**1:2:3**) in acetonitrile solutions for spin-coating of the single-doped and the double-doped host–guest films were 99.8 : 0.2 : 0 and 99.85 : 0.05 : 0.1, respectively. Since in LECs an ionic liquid BMIM⁺(PF₆⁻) of 20 wt.% was added to provide additional mobile ions and to shorten the device response time,²¹ the photophysical properties of the BMIM⁺(PF₆⁻) blended host–guest films were also characterized. The mass ratios of the solute component (**1:2:3:BMIM⁺(PF₆⁻)**) in acetonitrile solutions for spin-coating of the single-doped and the double-doped host–guest films containing BMIM⁺(PF₆⁻) were 79.8 : 0.2 : 0 : 20 and 79.85 : 0.05 : 0.1 : 20, respectively. The concentrations of all of the solutions for spin-coating were 70 mg mL⁻¹. PL spectra were measured with a fluorescence spectrophotometer (HITACHI F9500). PLQYs for solution and thin-film samples were determined with a calibrated integrating sphere system (HAMAMATSU C9920).

Fabrication and characterization of LEC devices

ITO-coated glass substrates (2 × 2 cm²) were cleaned and treated with UV/ozone prior to use. The PEDOT:PSS layer was spin-coated at 4000 rpm onto the ITO substrate in air and baked at 150 °C for 30 min. The emissive layer (~200 nm, as measured by profilometry) was then spin-coated at 3000 rpm from the acetonitrile solutions under ambient conditions. To reduce the turn-on time of the LEC device, the ionic liquid [BMIM⁺(PF₆⁻)] of 20 wt.% was added to enhance the ionic conductivity of the thin films.²¹ The mass ratios of the solute component and the concentrations of the solutions for spin-coating of the single-doped and the double-doped emissive layers were the same as those used for spin-coating of the single-doped and the double-doped host–guest films containing BMIM⁺(PF₆⁻) for the photophysical studies described above. After spin coating, the thin films were then baked at 70 °C for 10 h in a nitrogen glove box (oxygen and moisture levels below 1 ppm), followed by thermal evaporation of a 100-nm Al top contact in a vacuum chamber (~10⁻⁶ torr). The electrical and emission characteristics of the LEC devices were measured using a source-measurement unit and an Si photodiode calibrated with the Photo Research PR-650 spectroradiometer. All device measurements were performed under a constant bias voltage (2.9–3.3 V). The EL spectra were taken with a calibrated CCD spectrograph.

Acknowledgements

This work was financially supported by the National Science Council of Taiwan. The authors gratefully acknowledge Miss Ivy Chu of Keithley Instruments Inc. for supporting source-measurement units and Mr. Hsin-Huang Wu for assistance with the machinery of our experiment setup.

References

- 1 J. Kido, K. Hongawa, K. Okuyama and K. Nagai, *Appl. Phys. Lett.*, 1994, **64**, 815.
- 2 B. W. D'Andrade and S. R. Forrest, *Adv. Mater.*, 2004, **16**, 1585.
- 3 X. Gong, S. Wang, D. Moses, G. C. Bazan and A. J. Heeger, *Adv. Mater.*, 2005, **17**, 2053.
- 4 J. Huang, G. Li, E. Wu, Q. Xu and Y. Yang, *Adv. Mater.*, 2006, **18**, 114.
- 5 C. W. Tang and S. A. VanSlyke, *Appl. Phys. Lett.*, 1987, **51**, 913.
- 6 J. H. Burroughes, D. D. C. Bradley, A. R. Brown, R. N. Marks, K. Mackay, R. H. Friend, P. L. Burns and A. B. Holmes, *Nature*, 1990, **347**, 539.
- 7 Q. Pei, G. Yu, C. Zhang, Y. Yang and A. J. Heeger, *Science*, 1995, **269**, 1086.
- 8 Y. Yang and Q. Pei, *J. Appl. Phys.*, 1997, **81**, 3294.
- 9 M. Sun, C. Zhong, F. Li, Y. Cao and Q. Pei, *Macromolecules*, 2010, **43**, 1714.
- 10 J. K. Lee, D. S. Yoo, E. S. Handy and M. F. Rubner, *Appl. Phys. Lett.*, 1996, **69**, 1686.
- 11 C. H. Lyons, E. D. Abbas, J. K. Lee and M. F. Rubner, *J. Am. Chem. Soc.*, 1998, **120**, 12100.
- 12 F. G. Gao and A. J. Bard, *J. Am. Chem. Soc.*, 2000, **122**, 7426.
- 13 H. Rudmann and M. F. Rubner, *J. Appl. Phys.*, 2001, **90**, 4338.
- 14 H. Rudmann, S. Shimada and M. F. Rubner, *J. Am. Chem. Soc.*, 2002, **124**, 4918.
- 15 G. Kalyuzhny, M. Buda, J. McNeill, P. Barbara and A. J. Bard, *J. Am. Chem. Soc.*, 2003, **125**, 6272.
- 16 J. D. Slinker, D. Bernards, P. L. Houston, H. D. Abruña, S. Bernhard and G. G. Malliaras, *Chem. Commun.*, 2003, 2392.
- 17 H. Rudmann, S. Shimada and M. F. Rubner, *J. Appl. Phys.*, 2003, **94**, 115.
- 18 J. D. Slinker, A. A. Gorodetsky, M. S. Lowry, J. Wang, S. Parker, R. Rohl, S. Bernhard and G. G. Malliaras, *J. Am. Chem. Soc.*, 2004, **126**, 2763.
- 19 A. R. Hosseini, C. Y. Koh, J. D. Slinker, S. Flores-Torres, H. D. Abruña and G. G. Malliaras, *Chem. Mater.*, 2005, **17**, 6114.
- 20 J. D. Slinker, C. Y. Koh, G. G. Malliaras, M. S. Lowry and S. Bernhard, *Appl. Phys. Lett.*, 2005, **86**, 173506.
- 21 S. T. Parker, J. D. Slinker, M. S. Lowry, M. P. Cox, S. Bernhard and G. G. Malliaras, *Chem. Mater.*, 2005, **17**, 3187.
- 22 M. S. Lowry, J. I. Goldsmith, J. D. Slinker, R. Rohl, R. A. Pascal Jr., G. G. Malliaras and S. Bernhard, *Chem. Mater.*, 2005, **17**, 5712.
- 23 A. B. Tamayo, S. Garon, T. Sajoto, P. I. Djurovich, I. M. Tsyba, R. Bau and M. E. Thompson, *Inorg. Chem.*, 2005, **44**, 8723.
- 24 N. Armaroli, G. Accorsi, M. Holler, O. Moudam, J. Nierengarten, Z. Zhou, R. T. Wegh and R. Welter, *Adv. Mater.*, 2006, **18**, 1313.
- 25 H. J. Bolink, L. Cappelli, E. Coronado, M. Grätzel and M. Nazeeruddin, *J. Am. Chem. Soc.*, 2006, **128**, 46.
- 26 H. J. Bolink, L. Cappelli, E. Coronado, M. Grätzel, E. Ortí, R. D. Costa, P. M. Viruela and M. Nazeeruddin, *J. Am. Chem. Soc.*, 2006, **128**, 14786.
- 27 Q. Zhang, Q. Zhou, Y. Cheng, L. Wang, D. Ma, X. Jing and F. Wang, *Adv. Funct. Mater.*, 2006, **16**, 1203.
- 28 M. K. Nazeeruddin, R. T. Wegh, Z. Zhou, C. Klein, Q. Wang, F. De Angelis, S. Fantacci and M. Grätzel, *Inorg. Chem.*, 2006, **45**, 9245.
- 29 H. J. Bolink, L. Cappelli, E. Coronado, A. Parham and P. Stössel, *Chem. Mater.*, 2006, **18**, 2778.
- 30 H.-C. Su, F.-C. Fang, T.-Y. Hwu, H.-H. Hsieh, H.-F. Chen, G.-H. Lee, S.-M. Peng, K.-T. Wong and C.-C. Wu, *Adv. Funct. Mater.*, 2007, **17**, 1019.
- 31 H.-C. Su, C.-C. Wu, F.-C. Fang and K.-T. Wong, *Appl. Phys. Lett.*, 2006, **89**, 261118.
- 32 J. D. Slinker, J. Rivnay, J. S. Moskowitz, J. B. Parker, S. Bernhard, H. D. Abruña and G. G. Malliaras, *J. Mater. Chem.*, 2007, **17**, 2976.
- 33 L. He, L. Duan, J. Qiao, R. Wang, P. Wei, L. D. Wang and Y. Qiu, *Adv. Funct. Mater.*, 2008, **18**, 2123.

- 34 E. Z. Colman, J. D. Slinker, J. B. Parker, G. G. Malliaras and S. Bernhard, *Chem. Mater.*, 2008, **20**, 388.
- 35 H.-C. Su, H.-F. Chen, F.-C. Fang, C.-C. Liu, C.-C. Wu, K.-T. Wong, Y.-H. Liu and S.-M. Peng, *J. Am. Chem. Soc.*, 2008, **130**, 3413.
- 36 S. Graber, K. Doyle, M. Neuburger, C. E. Housecroft, E. C. Constable, R. D. Costa, E. Ortí, D. Repetto and H. J. Bolink, *J. Am. Chem. Soc.*, 2008, **130**, 14944.
- 37 H. J. Bolink, E. Coronado, R. D. Costa, E. Ortí, M. Sessolo, S. Graber, K. Doyle, M. Neuburger, C. E. Housecroft and E. C. Constable, *Adv. Mater.*, 2008, **20**, 3910.
- 38 H. J. Bolink, E. Coronado, R. D. Costa, N. Lardiés and E. Ortí, *Inorg. Chem.*, 2008, **47**, 9149.
- 39 H.-C. Su, H.-F. Chen, C.-C. Wu and K.-T. Wong, *Chem.–Asian J.*, 2008, **3**, 1922.
- 40 T.-H. Kwon, Y. H. Oh, I.-S. Shin and J.-I. Hong, *Adv. Funct. Mater.*, 2009, **19**, 711.
- 41 L. He, J. Qiao, L. Duan, G. F. Dong, D. Q. Zhang, L. D. Wang and Y. Qiu, *Adv. Funct. Mater.*, 2009, **19**, 2950.
- 42 C. Rothe, C.-J. Chiang, V. Jankus, K. Abdullah, X. Zeng, R. Jitchati, A. S. Batsanov, M. R. Bryce and A. P. Monkman, *Adv. Funct. Mater.*, 2009, **19**, 2038.
- 43 R. D. Costa, Enrique Ortí, H. J. Bolink, S. Graber, S. Schaffner, M. Neuburger, C. E. Housecroft and E. C. Constable, *Adv. Funct. Mater.*, 2009, **19**, 3456.
- 44 R. D. Costa, E. Ortí, H. J. Bolink, S. Graber, C. E. Housecroft, M. Neuburger, S. Schaffner and E. C. Constable, *Chem. Commun.*, 2009, 2029.
- 45 L. He, L. Duan, J. Qiao, G. Dong, L. Wang and Y. Qiu, *Chem. Mater.*, 2010, **22**, 3535.
- 46 R. D. Costa, E. Ortí, H. J. Bolink, S. Graber, C. E. Housecroft and E. C. Constable, *J. Am. Chem. Soc.*, 2010, **132**, 5978.
- 47 R. D. Costa, E. Ortí, H. J. Bolink, S. Graber, C. E. Housecroft and E. C. Constable, *Adv. Funct. Mater.*, 2010, **20**, 1511.
- 48 M. Mydlak, C. Bizzarri, D. Hartmann, W. Sarfert, G. Schmid and L. De Cola, *Adv. Funct. Mater.*, 2010, **20**, 1812.
- 49 H.-C. Su, Y.-H. Lin, C.-H. Chang, H.-W. Lin, C.-C. Wu, F.-C. Fang, H.-F. Chen and K.-T. Wong, *J. Mater. Chem.*, 2010, **20**, 5521.
- 50 C.-H. Yang, J. Beltran, V. Lemaire, J. Cornil, D. Hartmann, W. Sarfert, R. Fröhlich, C. Bizzarri and L. De Cola, *Inorg. Chem.*, 2010, **49**, 9891.
- 51 *Colorimetry*, Commission Internationale de l'Éclairage (CIE), Paris, 1986.
- 52 *Method of Measuring and Specifying Colour Rendering Properties of Light Sources*, Commission Internationale de l'Éclairage (CIE), Paris, 1974.
- 53 G. Wyszecki and W. S. Stiles, *Color Science - Concepts and Methods, Quantitative Data and Formulae*, Wiley Interscience, New York, 2nd edn, 2000.